 doi:10.20944/preprints201710.0014.v2

# Exploring Offshore Hydrothermal Venting Using Low-Cost ROV and Photogrammetric Techniques: a Case Study from Milos Island, Greece

**Teague, J.**[1*], Miles, J.[2,1], Connor, D.[1], Priest, E.[2], Scott, T.B.[1], Naden, J.[2], Nomikou, P.[3]

[1] **University of Bristol, Interface Analysis Centre (IAC), HH Wills Physics Laboratory, Tyndall Ave, Bristol, BS8 1TL, United Kingdom**

[2] British Geological Survey, Nicker Hill, Keyworth, Nottingham, NG12 5GG, United Kingdom

[3]University of Athens, Department of Geology and Geoenvironment, Panepistimioupoli Zografou, 15784 Athens, Greece

*Correspondence: Jt16874@bristol.ac.uk

**Keywords:** Hydrothermal; Venting; ROV; Photogrammetry; Greece; Milos.

Abstract

The study utilises two emerging low-cost technologies, low cost Remotely Operated Vehicle (ROV) and underwater photogrammetry techniques (Structure from motion (SfM)) using off the shelf cameras, for 3D reconstruction of shallow hydrothermal vent sites around Paleochori Bay, Milos Island, Greece. Venting fields were Characterised through interactive bathymetry models produced from still images taken from camera onboard ROV flown over areas of interest in double raster pattern.

This is the first time the shallow venting fields on Milos have been actively surveyed using the combined approach of ROV and photogrammetry. Areas were successfully surveyed and the bathymetry was reconstructed using SfM photogrammetry with a ~10 cm scale resolution. A diverse range of benthic habitats were surveyed and the resulting topographic models will act as a baseline for an established method, that given with positioning will provide further characterisation of the vent systems and any evolving seafloor morphology.

## 1 Introduction

This study provides an insight into modern-day hydrothermal venting observed immediately offshore (< 100 m) from the island of Milos in the Greek Cyclades.

The shallow submarine hydrothermal system of Milos island is an exemplar of a shallow hydrothermal system and has been extensively researched in term of its microbiological ecology and hydrothermal geochemistry. The island's high enthalpy geothermal field, observed at Zephyria, is considered to be the most important in Greece (Fytikas, Marinelli, 1976; Mendrinos et al., 2010).

Active hydrothermal venting in the shallow submarine environment (<100 m) is a relatively accessible environment to study magmatic-hydrothermal systems. Bubbles containing mixed $CO_2$,

Preprints (www.preprints.org) | NOT PEER-REVIEWED | Posted: 26 March 2018 doi:10.20944/preprints201710.0014.v2

$H_{2+}$, $H_2S$, and $CH_4$ gases escape from the seafloor in discrete zones, locally creating a hot and acidic environment. Often cooled by seawater mixing (to 60-12$^oC$; Fitzsimmons et al., 1997) prior to venting, the gases are initially transferred to the hydrothermal fluids from magma chamber degassing. Volatile species (e.g. Arsenic; As) and even metals (Fe, Cu, Pb, Ag and Au) may be dissolved into the hydrothermal fluids which contact the magma body. As the hot fluids circulate buoyantly upwards through the overlying rock strata, depressurisation and mixing with cooler pore waters causes a reduction in temperature and solubility of dissolved species, resulting in the exsolution of gases and precipitation of sulphide minerals such as pyrite ($FeS_2$) and chalcocite ($CuS_2$) at high temperature (<250$^oC$), and sulphate minerals at lower temperatures.

Seafloor bathymetry coupled with ROV derived imagery provides an excellent tool for elucidating geological features and structure of the seafloor. Studies (Bell *et al.,*2013, Carey *et al.,* 2011; Nomikou *et al.,* 2012, Sigurdsson *et al.,* 2006) have used ROV, whose capability reaches 3–4 km depth and deployed from large vessels, to help characterise and map submarine volcanoes or volcanic outcrops within the Hellenic Trench and the developed Aegean Volcanic Arc.

Though the ecology and geochemistry of the shallow submarine hydrothermal system on Milos are relatively well understood, the setting of discharges within the submarine landscape and their geological situation has not been studied to the same extent. This is because the shallow nature of the Milos hydrothermal significant parts of field (<50m) precludes the deployment of most ship- and AUV-based bathymetric and other submarine surveying equipment.

Therefore, a shallow easily deployed system is required, such as a 'low cost' remotely operated vehicle (ROV). An ROV is essentially a tethered underwater robot. The total ROV system is comprised of the vehicle, which is connected to the control circuit and the operators on a stable platform (boat or shore) by a tether or umbilical - a group of cables that convey video and data signals between the operator and the vehicle. Currently the most available 'low cost' ROV's range from ~£500 - £30,000 (largely dependant on the systems and sensors onboard). Within this range, the depth limit is typically 100m which encompasses shallow systems.

Here we utilise a low cost ROV to provide the first detailed examination of three shallow (<10 m) vent fields in Paleochori Bay, Milos and provide <1 m bathymetry of selected areas of the hydrothermal field. Hence demonstrating the efficiency of the technology for exploring a range of geological features in this environment.

### 1.1 Milos geology and geothermal activity

Milos is the most south-westerly island in the Cyclades archipelago (Fig. 1). Located in the South Aegean Active Volcanic Arc (SAAVA), Milos is generally accepted as an example of an emerged volcanic edifice (1.4 Ma; Stewart and McPhie, 2006) created from monogenetic pulses of effusive and explosive magmatism, but has remained dormant for the last 90 kyr (Fytikas, 1986). The SAAVA is the surface expression of active, northward subduction of the African plate beneath the Aegean microplate and consequential slab rollback as the tectonic regime switched to extensional (Jackson, 1994). The arc spans a maximum of 200 km wide, from Crommyonia in the west, through Methana, Aegina, Milos, Santorini, to Nisyros and Kos in the east (Innocenti *et al.,* 1979; Fytikas *et al.,* 1984; Stewart and McPhie, 2006). The island of Milos is the largest worldwide exporter of bentonite, and is home to a significant range of metal and non-metalliferous mineral deposits. It is a preserved on-land laboratory to study hydrothermal ore-forming processes from the shallow submarine

Preprints (www.preprints.org) | NOT PEER-REVIEWED | Posted: 26 March 2018 doi:10.20944/preprints201710.0014.v2

environment. The associated shallow submarine hydrothermal venting fields are far less studied in the same detail.

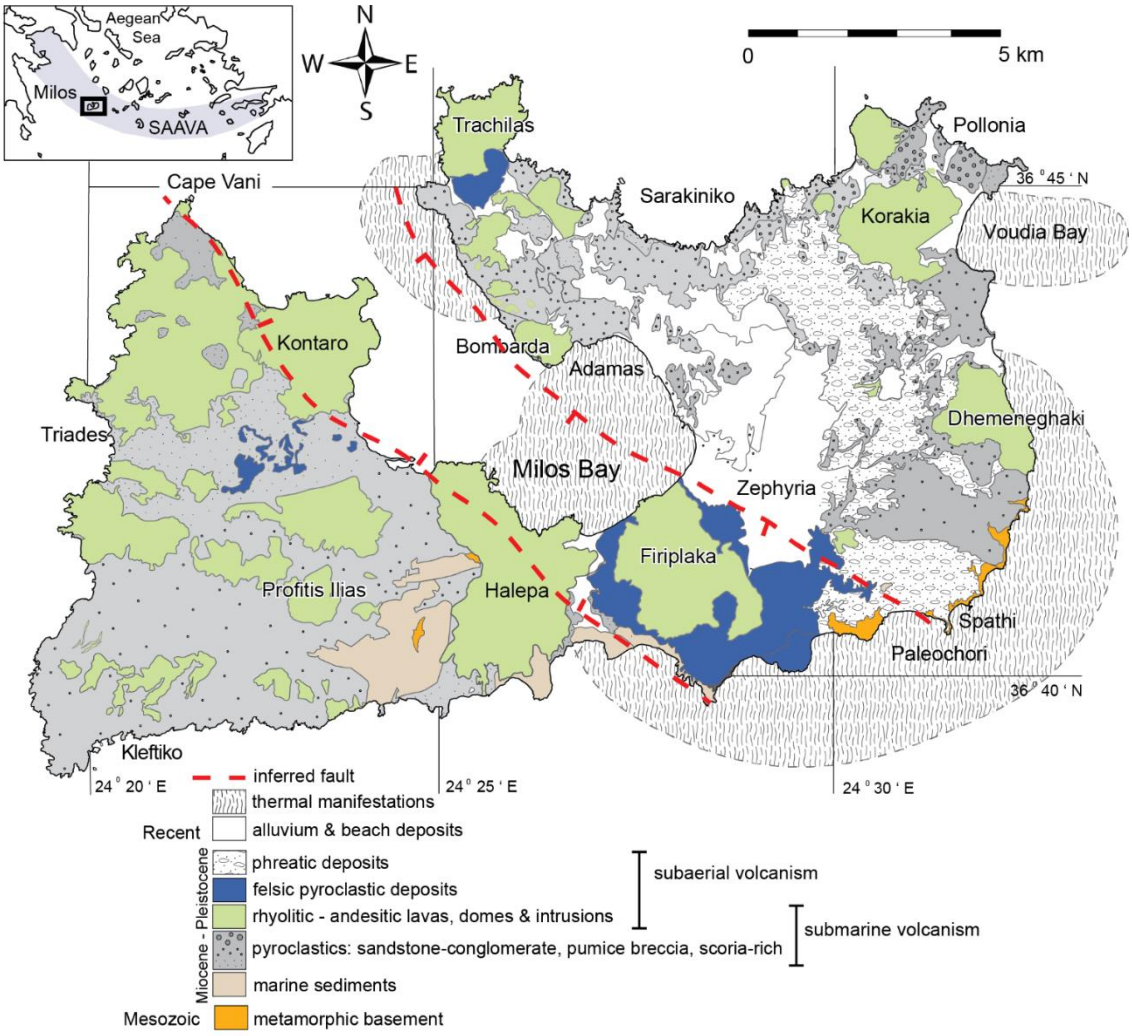


**Fig. 1: Geological map of Milos island, Greece, with known thermal manifestations. Extent of hydrothermal activity is approx. 34 km$^2$. Modified from Stewart & McPhie, 2006 and Gilhooly et al., 2014.**

In the near-shore environment, the most intense venting activity (0–15 m water depth) is located along the SE coastline at Paleochori Bay nearby the subaerial Firiplaka volcanic crater (Dando *et al.,* 1995d; Cronan and Varnavas, 1999; Nomikou *et al.,* 2013). Three other zones identified from the 2010 Volcanism Program (ID number #0102-03) include (1) within Milos Bay; (2) the entrance to Milos Bay; and (3) Voudia Bay (Dando, 2010; Fig 2). Within these zones, continuously degassing vents are heterogeneously scattered within discreet areas associated with intensively fractured regions of the seafloor (Dando *et al.,* 1995b; Price *et al*., 2009). Activity has also been identified at greater depths (70–300 m) by use of echo sounders and transducers used to detect sonic scatter caused by bubbling (Dando *et al.,* 1995a, b; Valsami-Jones *et al*., 2005). The observed zones of hydrothermal activity correspond with the prolongation of the eastern marginal fault of the neotectonic graben, which hosts the Firiplaka sub-aerial volcano (Fig. 2; Papanikolaou *et al.,* 1990).

Within the near-shore submarine environment of Milos, microbial mats and mineral precipitates (varying white, orange and yellow) are observed in the vicinity of active venting sites (Sievert *et al.,* 1999). Within the different coloured zones of mineral precipitation, significant aberrations in pH, temperature, $H_2S$ content and alkalinity contrast have been reported (Yücel *et al.,* 2013). The pore

Preprints (www.preprints.org) | NOT PEER-REVIEWED | Posted: 26 March 2018 doi:10.20944/preprints201710.0014.v2

fluids within the zones of white mineral precipitation reveal a pH of 4.8-5.4, temperatures of 49-71°C, $H_2S$ concentrations of 0.24-2.85 mM and alkalinity of 920-3400 mM/kg. In contrast, zones of orange and yellow mineral deposits exhibit slightly more acidic conditions (pH 4.6-5.1) and higher vent temperatures (71-95°C) with higher $H_2S$ concentrations (3.1 mM) and reduced alkalinity 778 mM/kg (Yücel *et al.,* 2013). Fluids analysed from venting at Paleochori Bay (approx. 36"N 40.30'N 24" 31.25'E) revealed venting of less harshly acidic fluids (pH 5.3-7.6), with variable temperatures (26-116°C) and containing As-rich gases and fluids (Fitzsimmons *et al.,* 1997), attributed to the leaching of the pyrite veins of the greenschist basement rocks (Price et al., 2013). The gas phase is composed mainly of $CO_2$ (92.5 %) and $H_2S$ (6.7 %), with lesser amounts of $O_2$ (0.13 %), $N_2$ (0.67 %), $H_2$ (11450 ppm), $CH^4$ (916 ppm), He (7 ppm) and CO (0.7 ppm) (Botz et al., 1996; Price et al., 2013).

## 2 Survey Location (Paleochori Bay)


Fig. 2: The surveyed site of Paleochori bay on the south-eastern side of Milos island. (Google Earth, 2017)

The location of Paleochori Bay, located on the south-eastern side of Milos island (Fig. 2), was chosen for a shallow survey due to the continuous release of gas bubbles observed on the shallow seafloor (Valsami-Jones, *et al*. 2005), visible at the sea surface when sea conditions are calm. Due to the close proximity of these venting sites to the Milos shoreline, this site is ideally placed for being studied by low-cost remotely operated vehicle (ROV) systems piloted from land as opposed to by boat.

The bay is approximately 0.8 km long and the area around the beach is lightly industrialized. High tide at the time of study was around 0200h and 1400h with low tides at 0800h and 2000h, and a shift of 0.12 m. The ROV deployments were made over three days (23-25$^{th}$ May 2017), in three separate sites within Paleochori Bay (Fig. 3).

The three sites where the ROV was deployed from (on shore):

- Pilot survey (A): ROV survey Launch position (24.518727, 36.674524) middle of survey area (24.516348, 36.674429), approx. area surveyed (1,485m$^2$). Beaufort state: 1, Start Time: 09:25, End Time: 10:15, Tide: Low. Initial testing and calibration of the ROV was performed to verify suitable buoyancy, manoeuvrability and sufficient propulsion capability to overcome tidal currents. The ROV was used to rapidly scout the bay area to locate sites of active seafloor venting.

- Survey 1 (B): East end of Paleochori Bay (36.674432, 24.521813), middle of survey area (24.516348, 36.674429), approx. area surveyed (1,040m$^2$). Beaufort state: 2, Start Time: 08:30, End Time: 9:00, Tide: Low. Directly S/SE of active cliff-face fumaroles located along the bay's coastline and on the inferred NW-SE trending horst-graben fault (Fytikas, 1997; Fig. 1).

*Preprints* (www.preprints.org) | NOT PEER-REVIEWED | Posted: 26 March 2018 doi:10.20944/preprints201710.0014.v2

- Survey 2 (C): West end of Paleochori Bay (36.675022, 24.516856), middle of survey area (24.521797, 36.673995), approx. area surveyed (1,290m$^2$). Beaufort state: 2, Start Time: 10:25, End Time: 11:10, Tide: Low. Similar to Survey 1, deployment was influenced by the location of active on-land fumaroles. Local Milians advised where would be best to deploy.

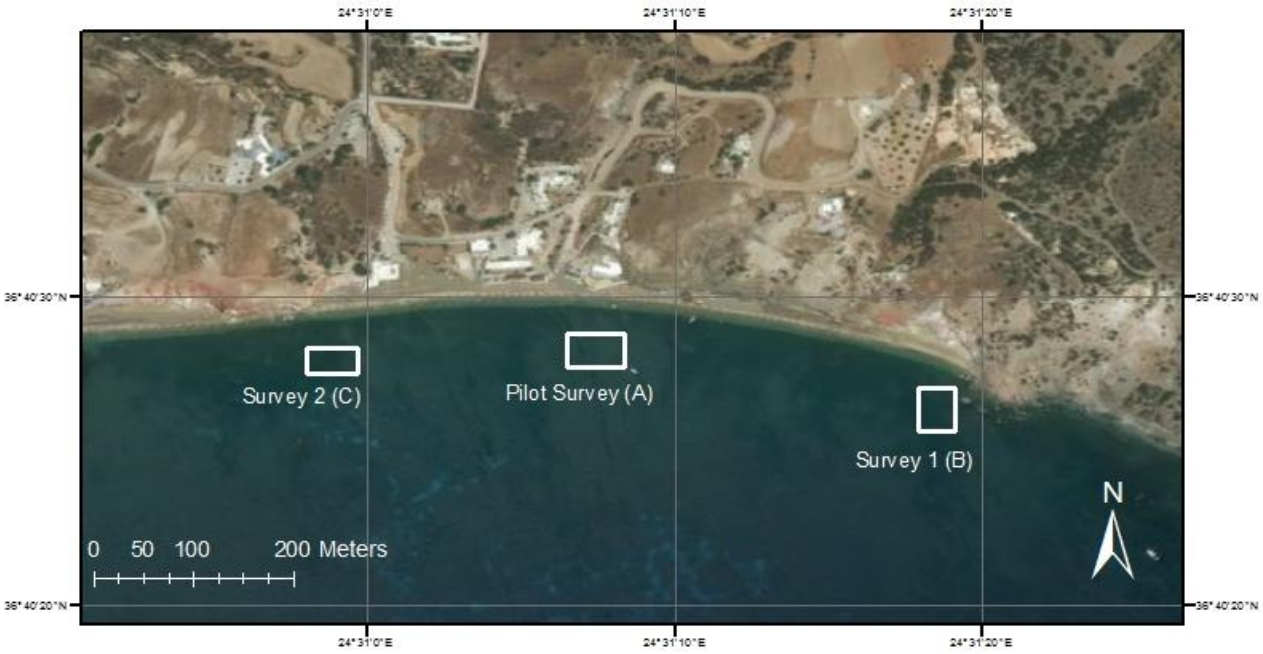


**Fig. 3: ROV survey sites at Paleochori Bay, Milos: (A) Pilot survey south of Pits Watersports; (B) Survey 1 eastern end of Paleochori Bay; (C) Survey 2 western side of bay, in front of local tavern. (Google Earth, 2017).**

## 3 Methodology

Preliminary reconnaissance was undertaken by snorkeling from the surface and using on land geological features such as faults, and sulfur discolourations. The ROV was used to subsequently map areas of venting in more detail.

The ROV (model BlueROV2; Fig. 4) was equipped with a HD video camera and operated from an onshore laptop (standard Windows/Mac operating system and latest version of Qground control) providing sight and controls.

The ROV is connected to the surface through a 100 m umbilical tether that serves for data communication and real-time video transmission. Six thrusters contribute to give vectored thrust, four on each of the corners and two at the top of the ROV to give forward/backwards, left/right and upwards/downward movements, respectively, when in operation.

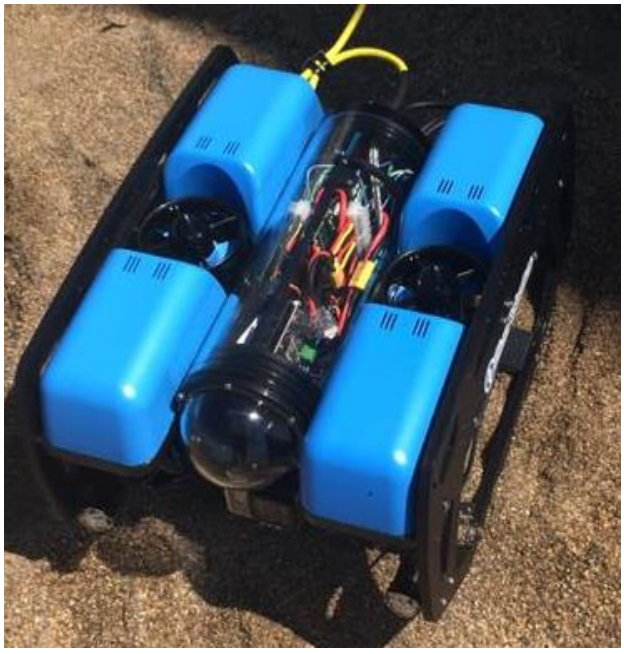

**Fig. 4: BlueROV2, Length 457mm x Width 338mm x Height 254mm.**

Preprints (www.preprints.org) | NOT PEER-REVIEWED | Posted: 26 March 2018 doi:10.20944/preprints201710.0014.v2

The use of Structure-from-Motion (SfM) photogrammetry, which is an emerging low-cost photogrammetric method for high-resolution 3D topographic reconstruction, was used to enable production of digital elevation models (DEMs) for each venting site surveyed. Such models can be analysed using topographic software tools such as ArcGIS which enables structural metrics to be quantified such as surface complexity (3D/2D surface area), slope, and curvature (Burns *et al. 2015*).

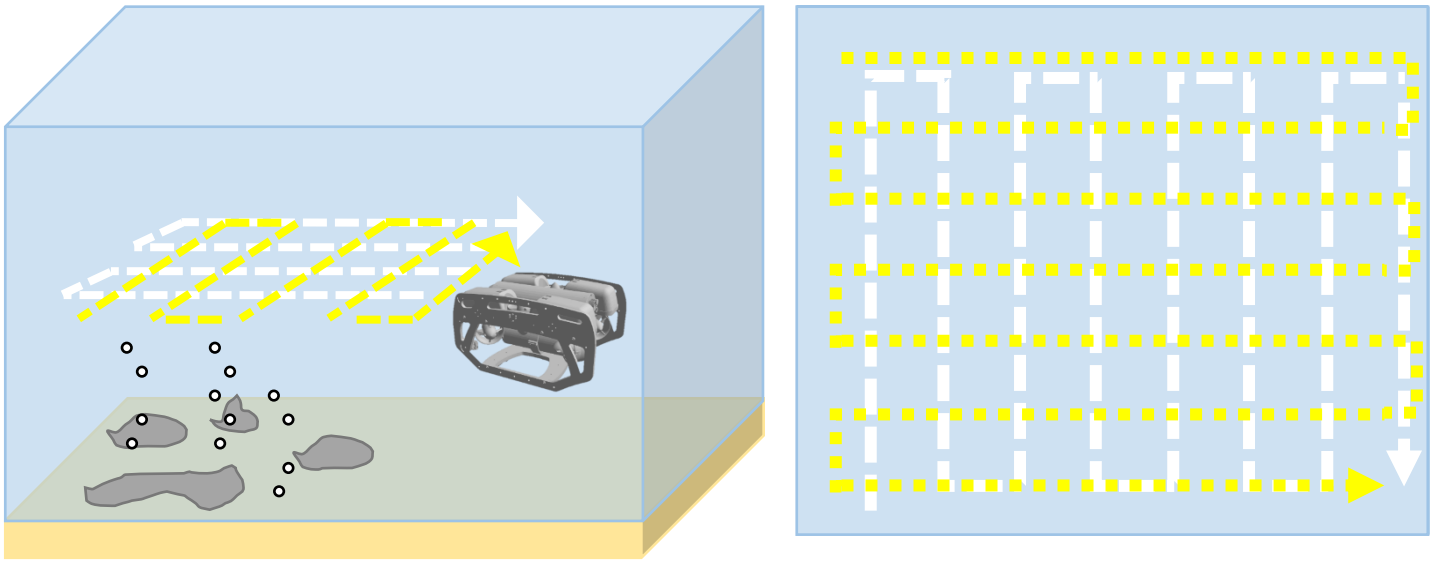

Fig. 5: (A) 3D representation of raster pattern over vent field showing camera field of view. (B) Top down view of raster pattern survey.

The ROV photogrammetric survey of the seafloor is achieved by manually 'flying' in two intersecting raster patterns (Fig. 5; Teague and Scott, 2017), maintaining a 1 m approx. distance from the seabed using the ROVs build-in depth hold feature. The attached HD camera took visual data in the form of either a video or time-lapse, a similar approach to established unmanned aerial vehicle (UAV) photogrammetry techniques, allowing for sufficient overlap of images between transects. In order to obtain the photos, a HD waterproof camera (GoPro Hero 5), was mounted to the ROV facing directly down at the seafloor. The camera was set to record an image every 0.5 seconds to ensure maximum overlap between images. An acceptable level of overlap to gain a quality photogrammetric model is considered to be approximately 80 % between on-lapping (overlapping images in the direction of flight) images and 60 – 80 % between side-lapping (overlapping images perpendicular to the direction of flight) images (Colomina and Molina, 2014). Each survey site block was explored for approx. 40 minutes, where mapping and identification of venting sites was undertaken. Recovery of the ROV took 10-15 minutes, retrieved by towing it back to shore using the tether.

Once data was obtained, images are added to Agisoft Photoscan to make 3-dimensional models. This program uses the process structure from motion (SfM) photogrammetry. Studies (Snavely et al., 2008; Westoby *et al.,* 2012) indicate the principle advantage of SfM is the geometry of the surveyed area, the varying camera positions, and orientations without the need for georeferenced targets since GPS does not work underwater.

Agisoft Photoscan is widely regarded as an 'autonomous process' for creating 3D models, requiring small inputs from the user in order to achieve a basic model. A generalised workflow explains the following processing chain (Fig. 6;Agisoft, 2016). The software begins by aligning the input images (6-11 hours processing) to create a point cloud (1-4 hours). A point cloud is a three-dimensional

 doi:10.20944/preprints201710.0014.v2

coordinate system, defined by X (horizontal), Y (vertical), and Z (height) coordinates. The next step is to produce a dense cloud (15-40 minutes) based on estimated camera positions. Agisoft Photoscan calculates the camera depth and incorporates this information into a single dense point cloud. A solid mesh model is created and then shaded (5- 20 minutes), to create the morphology of the reconstruction. The final step is to apply texture (5-10 minutes) to the model. Agisoft Photoscan overlays the photomosaic onto the textured model to produce the final 3D model of the site surveyed. The models were processed on a Dell Alienware 15 laptop (Intel® Core™ i5-7300HQ: Quad-Core, 6MB Cache, up to 3.5GHz w/ Turbo Boost, RAM: 8GB DDR4 at 2400MHz (1x8GB)).

Photoscan uses a series of algorithms to create an initial sparse point cloud detecting features on a series of reference images and then matching these to corresponding features with subsequent images. Features with highly probable matches present in a number of images, a least squares estimate is applied and any outliers removed from the match process (AgiSoft, 2012).

A similar process is used in the Scale Invariant Feature Transform (SIFT) algorithm proposed by Lowe (2004), with modifications (Gonçalves and Henriques, 2015). With the linked sets of points between images identified and optimised, a network bundle adjustment algorithm is then applied. This algorithm provides the optimal 3D scene geometry using the estimated 3D scene coordinates, the camera poses and their calibrations (Triggs *et al.,* 2000; Conner *et al.,* 2017).

Preprints (www.preprints.org) | NOT PEER-REVIEWED | Posted: 26 March 2018 doi:10.20944/preprints201710.0014.v2

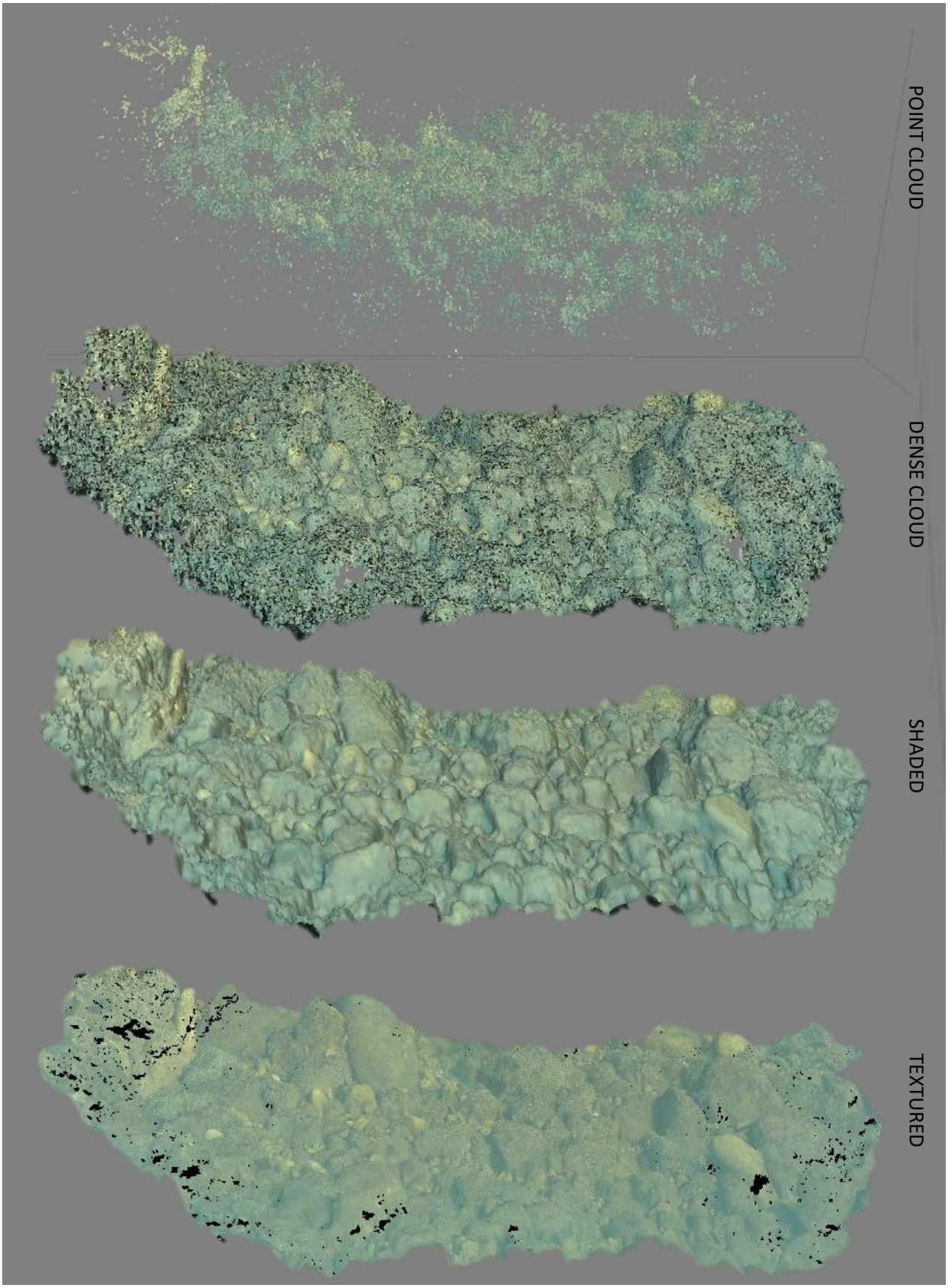


**Fig. 6: The photogrammetry processing steps in order: (1) point cloud, (2) dense cloud, (3) shaded and finally (4) textured. The time taken for this full process varies dependant on number of images as quality rendered. Processed data from Venting field 1.**

*Preprints* (www.preprints.org) | NOT PEER-REVIEWED | Posted: 26 March 2018 doi:10.20944/preprints201710.0014.v2

## 4 Results

Underwater venting at survey sites B and C were identified by continual gas bubbling observed at depths between 2 and 5 m (Fig. 7). Each entire survey area was not mapped, only areas displaying venting where mapped. Once located, the venting fields were mapped to create 3D reconstructions highlighting the bathymetric morphological structure of Survey 1 (B; Figs. 8 & 9) and Survey 2 (C; Figs. 10, 11 & 12).

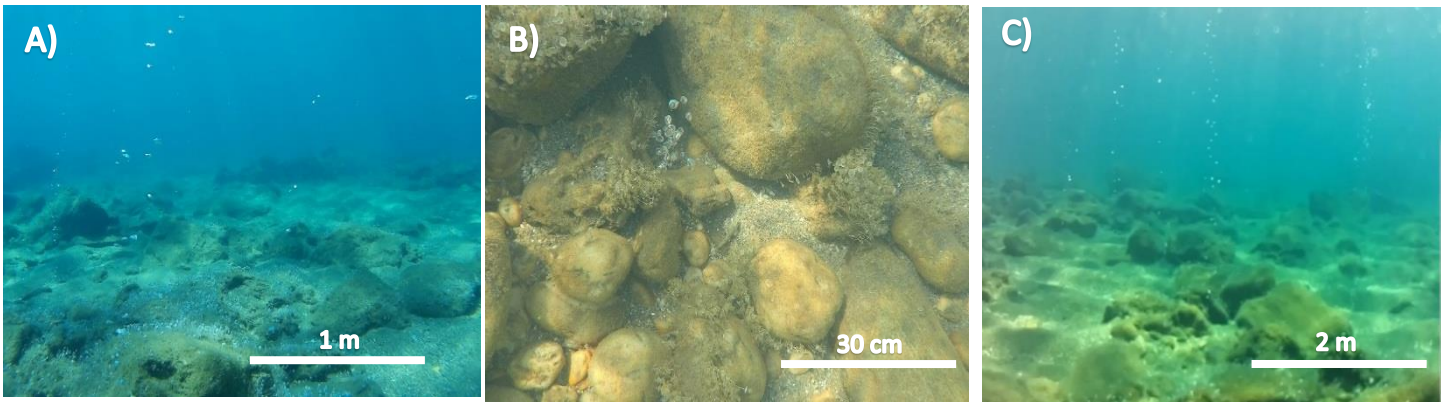


**Fig. 7: Still images of the vents at both sites to show the bubble columns not visible on photogrammetry. A) venting field 2 B) venting field 1 on top of a column C) slightly west of venting field 5. Images taken using the ROVs main forward-facing camera.**

Preprints (www.preprints.org) | NOT PEER-REVIEWED | Posted: 26 March 2018 doi:10.20944/preprints201710.0014.v2

### 4.1 Survey 1 (Site B Fig.3)

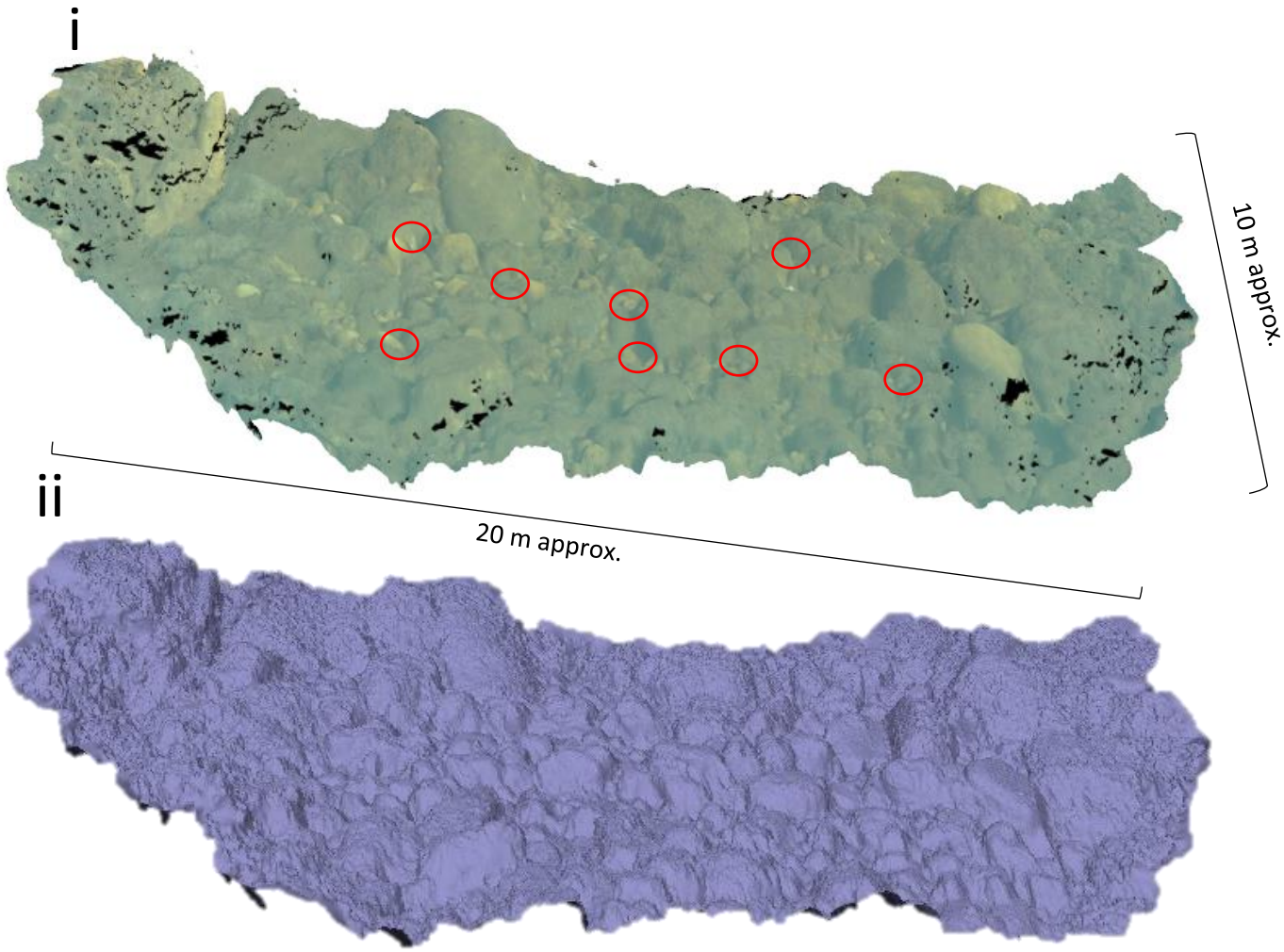


Fig. 8: Venting field 1: i) orthographic model processed from 799 images (GoPro Hero 5) 46,783 data points. 9573 X 10719 pixels; ii) un-textured model showing the bathymetry. Area of low energy infralittoral rock (EUNIS habitat type A1.3), with venting occurring through cracks or gaps in the rock outcrops. Highlighted in red, areas of observed venting activity.

*Preprints* (www.preprints.org) | NOT PEER-REVIEWED | Posted: 26 March 2018 doi:10.20944/preprints201710.0014.v2

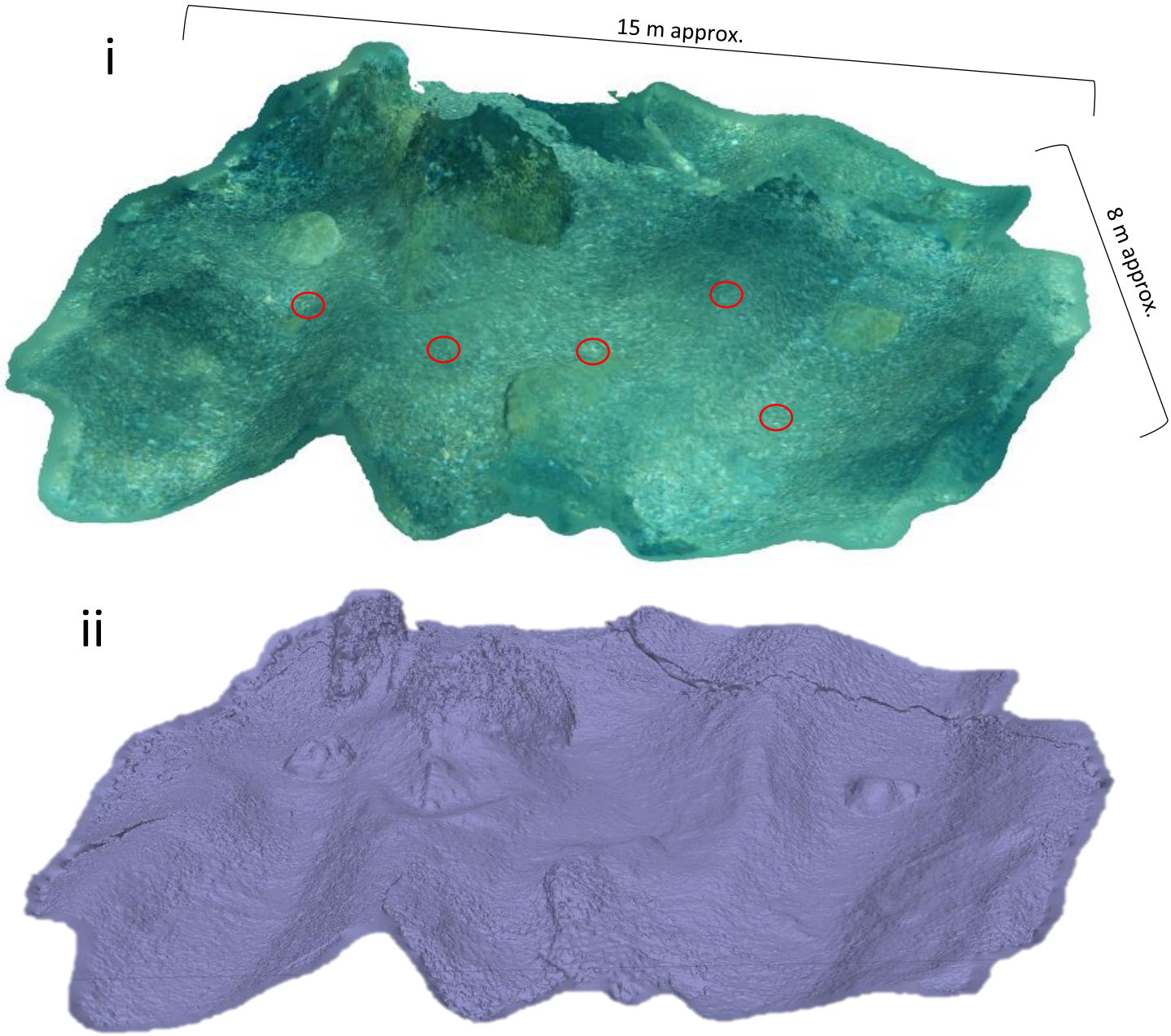


**Figure 9: Venting field 2: i) orthographic model Processed from 1064 images (GoPro Hero 5) 37,876 data points. 9055 x 8909 pixels. ii) un-textured model showing the bathymetry. Area of mediolittoral coarse detritic sediment (EUNIS habitat type A2.13). With venting occurring through sand. Highlighted in red, areas of observed venting activity.**

Preprints (www.preprints.org) | NOT PEER-REVIEWED | Posted: 26 March 2018 doi:10.20944/preprints201710.0014.v2

### 4.2 Survey 2 (C fig.3)

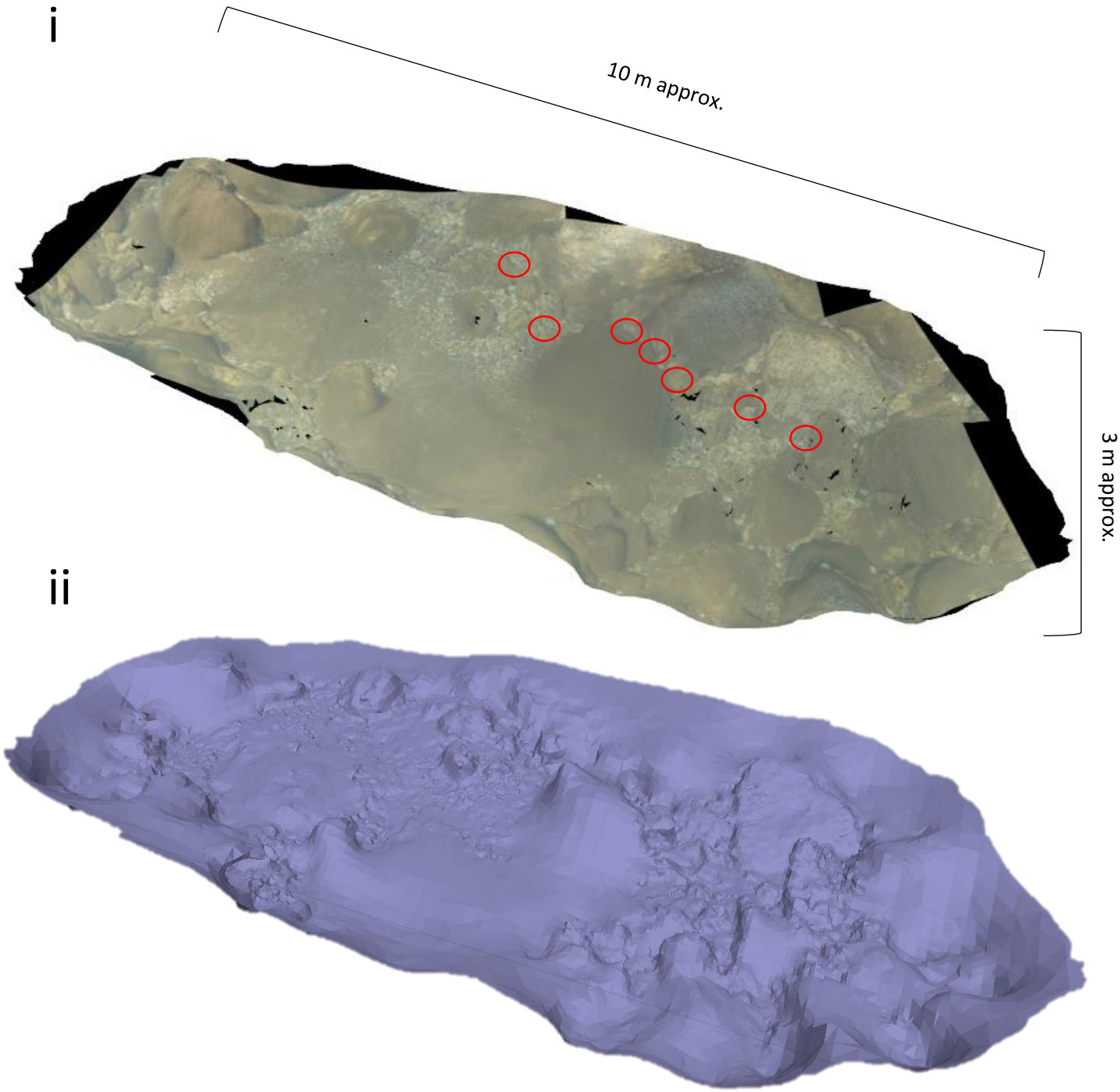


Fig. 10: Venting field 3: i) orthographic model processed from 149 images (GoPro Hero 5) 39,858 data points. 13339 x 7737 pixels. ii) un-textured model showing the bathymetry. Area of low energy infralittoral rock (EUNIS habitat type A3.3). With venting occurring through sand and gaps in rock outcrops. Highlighted in red, areas of observed venting activity.

*Preprints* (www.preprints.org) | NOT PEER-REVIEWED | Posted: 26 March 2018 doi:10.20944/preprints201710.0014.v2

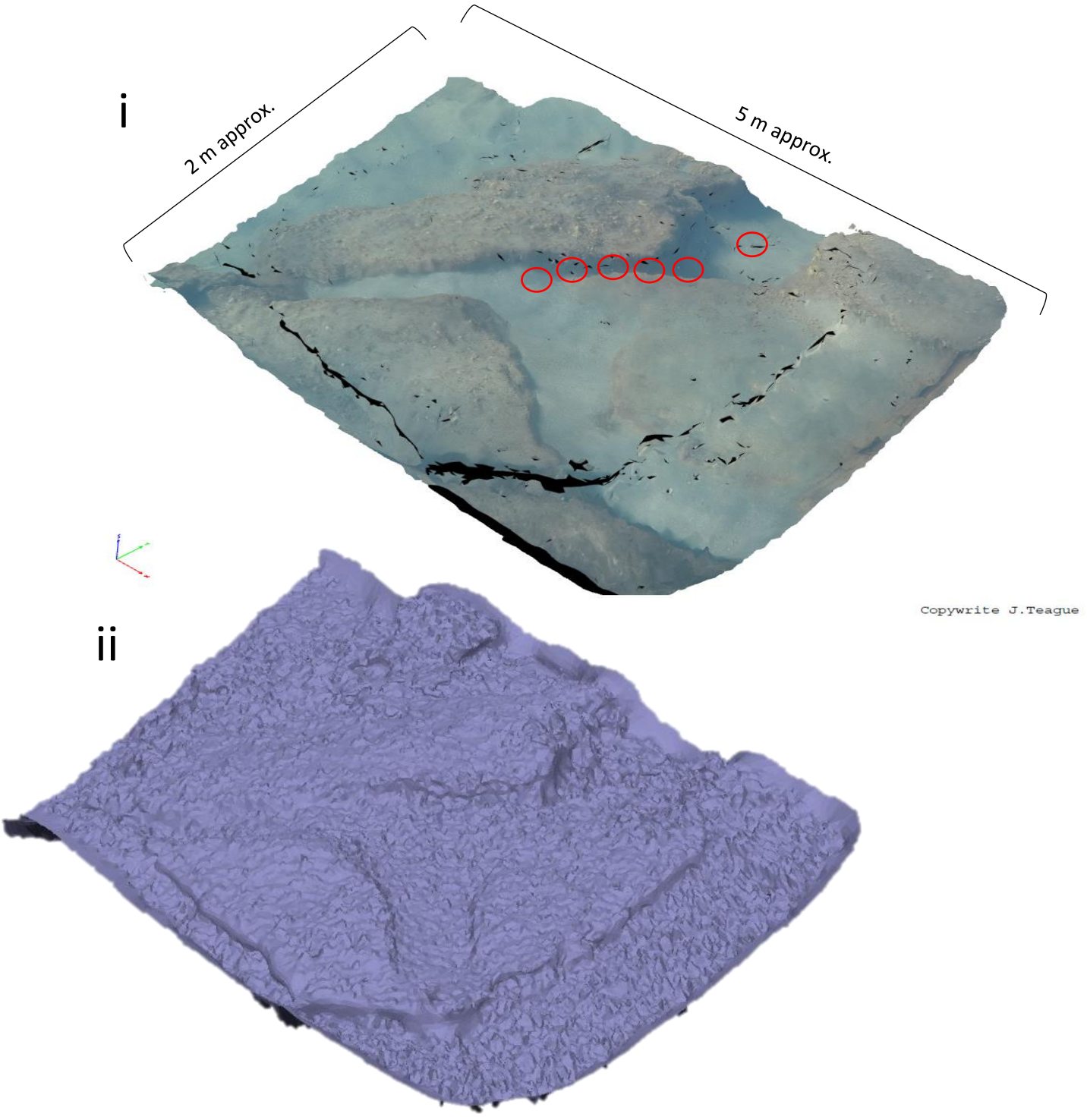


**Fig. 11: Venting field 4: i) orthographic model Processed from 187 images (GoPro Hero 5) 600 data points. 4619 x 3326 pixels. ii) un-textured model showing the bathymetry. Area of low energy infralittoral rock (EUNIS habitat type A3.3). With venting occurring through gaps in rock outcrops. Highlighted in red, areas of observed venting activity.**

Preprints (www.preprints.org) | NOT PEER-REVIEWED | Posted: 26 March 2018 doi:10.20944/preprints201710.0014.v2

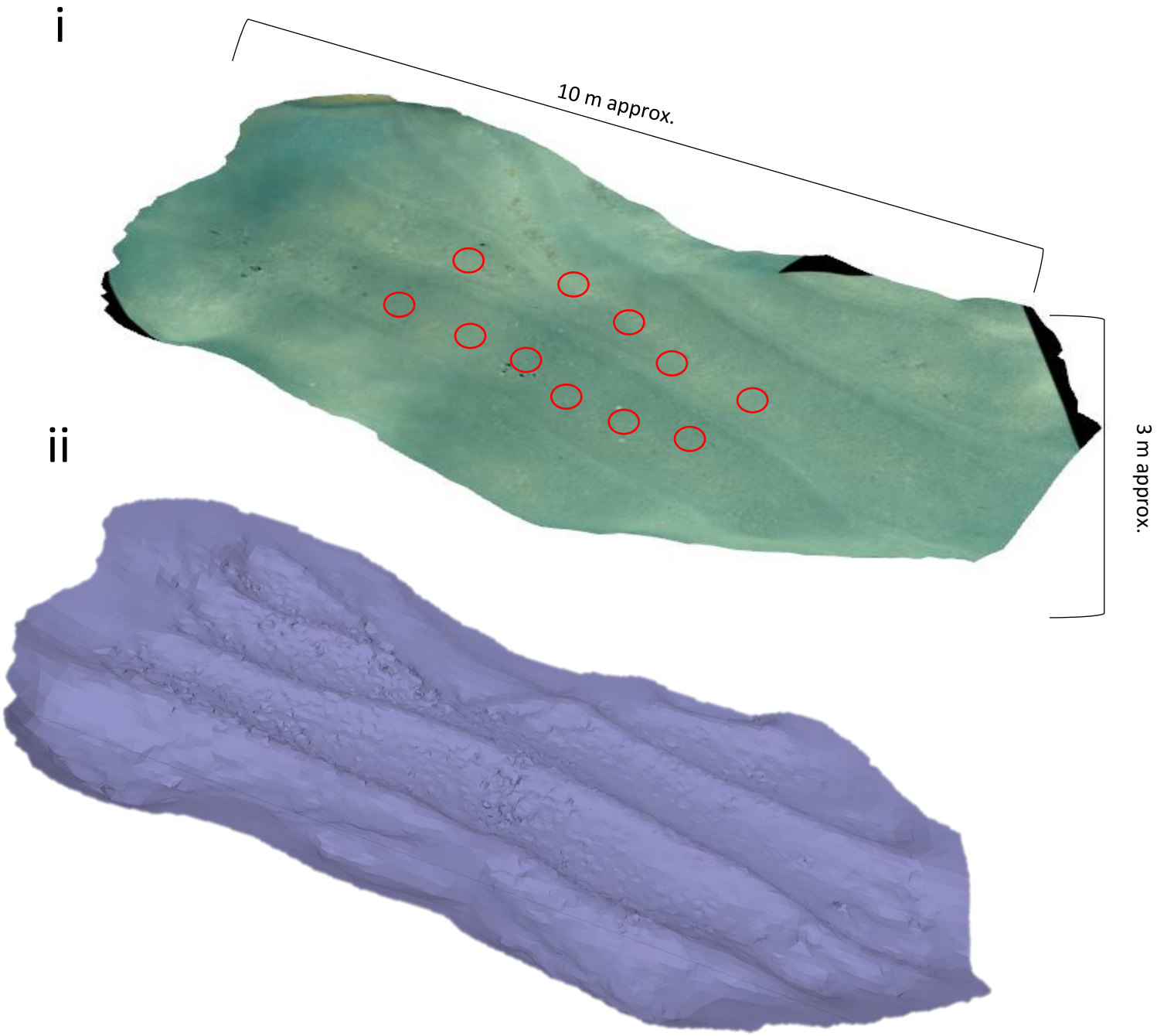


**Fig. 12: Venting field 5: i) orthographic model Processed from 368 images (GoPro Hero 5) 35,862 data points. 8637 x 7129 pixels. ii) un-textured model showing the bathymetry. Area of low energy littoral sand (EUNIS habitat type A2.2). With venting occurring through sand. Highlighted in red, areas of observed venting activity.**

## 5 Discussion

Shallow submarine (<7 m) venting fields were successfully mapped and modelled at 2 sites located along Paleochori Bay. These resulting topographic models indicate that the active shallow venting fields are not exhibiting any significant mineral accumulations at the seafloor surface as indicated in previous studies. This would be expected based on the relatively low temperatures previously indicated for the venting plumes (Yücel et al., 2013; Fitzsimmons et al. 1997), which indicates that

*Preprints* (www.preprints.org) | NOT PEER-REVIEWED | Posted: 26 March 2018 doi:10.20944/preprints201710.0014.v2

the majority of mineral precipitation would have occurred at much higher temperatures (>100°C) within the deeper rock strata of the seafloor.

This is the first time the venting fields have been actively surveyed using ROV based photogrammetry. This is a more effective method than traditional scuba based techniques as an ROV can cover more ground in less time than a diver. A dive survey is dependent on the air tank used (standard air tank 12L/ 200 bar, lasts approximately 1 hour at 10 m depth). ROV surveys are dependent on battery life, of which multiple sets can be used to extend time, notably the ROV doesn't fatigue unlike divers (Teague & Scott, 2017). Using the study of Robinson *et al*. (1997) as a comparison, 94 dives were undertaken by 11 divers over a 14-day period, duration ranging from 5 to 120 minutes (mean duration 35 minutes). Using the mean dive time, 54.83 hours were spent mapping a 500 $m^2$ block. By comparison, 3 dives with the ROV were undertaken by 2 people over a 3-day period with a duration of 41 minutes. With a total of 3.33 hours spent mapping an approximate area of 390 $m^2$ prior to processing. Using the average of the data processing steps, it takes approx. 10 hours to create each of the 5 models produced, totaling the time to 53.33 hours - a similar time taken previously by scuba divers (Robinson et al., 1997), however at much higher resolution with a 3D texture.

The resulting topographic models for the venting sites will act as a baseline methodology for future studies which will further characterise the vent systems and evolving seafloor morphology associated with mineral deposition. The approximate locations of the gas venting were derived from the still images used to generate the models; this could be made more accurate by the addition of another camera facing forward on the ROV or through use of echo-sounders or side-scan sonar to pinpoint exact locations. However, the use of these sensors would increase the cost associated with the technique. The current photogrammetry method is unable to generate the bubble columns from venting sites as they are not a consistent feature, especially as large areas were surveyed and therefore cannot be rendered in 3D. As shown by the raw solid models, we can survey and accurately reconstruct the bathymetry of the venting fields using SfM photogrammetry with a ~10 cm scale resolution. This also allows for quick identification types of benthic structures and habitats distinctions, this could be later used when charactersing venting bathymetry to draw similarities between sites. Compared with traditional bathymetric profiling methods e.g. side-scan sonar and LiDAR bathymetry, the photogrammetric method of surveying costing substantially less to procure and deploy. Unlike other methods, it can be conducted in shallow environments where larger robots cannot go such as Autonomous Underwater vehicles (AUVs). Sidescan sonar typically costs around £25k+ (BlueView M900 Series) meaning that simple photogrammetry (camera + software) costs 25 times less than traditional sonar and side scan methods.

The challenges of the underwater environment include the turbidity of water. The presence of suspended particles means operators work on large data sets, much closer to objects being surveyed (between 0.5 and 2 to 3 m, depending on the water quality; Drap, 2012; Teague & Scott, 2017). The technique presented relies on the survey being conducted in 'shallow' systems, the reason is twofold; firstly, the photic zone where light is abundant, is required to illuminate the survey area to be imaged. This survey technique could however be implemented in the aphotic zone with a few modifications including using the ROV LEDs to flash at the same time of imaging, the camera and strobing would need to be synchronised. Using flash would conserve power and would ensure an even illumination of the area of the seafloor being surveyed. Secondly, the camera (GoPro Hero 5, in

super suit housing) is only suitable for depths no greater than 60 m. Therefore, at greater depths, an alternative pressure resistant waterproof housing would be required.

The transect lines used in the raster pattern for surveys were created manually, since GPS does not work underwater and underwater positioning is costly. The raster lines were made using the ROVs telemetry data, such as the depth and compass heading and underwater land marks to signal the end of lines. The lines could be shown by timestamping the visual data from the ROV cockpit and recording the ROVs telemetry data or alternatively by using underwater positioning.

Further work would include (i) mapping larger areas of Paleochori Bay, moving further offshore in search of deeper vent sites, and (ii) using a boat as the platform in which we deploy from. Other sites surrounding the Milos coastline will also be explored e.g. Spathi Bay, to find higher temperature venting where active seafloor mineral accumulation is more obviously occurring. It would then be possible to draw a comparison to the bathymetry of the venting sites presented here to further understand the patterns and changes in the morphology of these systems with time. To make these future surveys more comprehensive, the ROV system will be fitted with a 'cats whiskers' thermocouple array and gas sampling apparatus, based on a modified version of a Niskin Bottle, such that vent temperatures and compositions may be compared between different sites of hydrothermal fluid release, both on and offshore. The use of Underwater GPS systems such as a Short baseline (SBL) system, offers a mobile low cost solution as SBL systems do not require any seafloor mounted transponders and therefore suitable for tracking underwater ROV from mobile platforms such as boats or ships that are either stationary or moving. SBL works by connecting three or more individual sonar transducers by wire to a central control box which send out pings to the object being tracked. By working out speed of transition & angle, the master board calculates the position of any locator relative to the position of the receivers. Combined with the integrated GPS and IMU, it provides an accurate GPS position of the Locator attached to the ROV (Waterlinked, 2017).

## 6 References

AgiSoft.(2012). *AgiSoft PhotoScan User Manual - Professional Edition,* Version 0.9.0.

Agisoft.(2016). *Agisoft PhotoScan User Manual: Professional Edition, Version 1.2.*

Bell, K.L.C., Carey, S.N., Nomikou, P., Sigurdsson, H., Sakellariou, D. (2013). Submarine evidence of a debris avalanche deposit on the eastern slope of Santorini volcano, Greece. *Tectonophysics*, **597**, pp.147-160.

Botz, R., Stüben, D., Winckler, G., Bayer, R., Schmitt, M., Faber, E. (1996). Hydrothermal gases offshore Milos Island, Greece. *Chemical Geology*, **130(3-4)**, pp.161-173.

Burns J.H.R., Delparte D., Gates R.D., Takabayashi M. (2015). Integrating structure-from-motion photogrammetry with geospatial software as a novel technique for quantifying 3D ecological characteristics of coral reefs. *PeerJ*, **3**, pp.1077.

Carey, S., Bell, K.L.C., Nomikou, P., Vougioukalakis, G., Roman, C., Cantner, K., Bejelou, K.,Bourbouli, M., Martin Fero, J.(2011). Exploration of the Kolumbo volcanic rift zone. *Oceanography,* **24 (1),** pp.24–25.

Camilli R., Sakellariou D., Foley B., Anagnostou C., Malios A., Bingham B., Eustice R., Goudreau J., Katsaros K. (2007). Investigation of Hydrothermal Vents in the Aegean Sea using an Integrated Mass Spectrometer and Acoustic Navigation System Onboard a Human Occupied Submersible, in: *Rapp. Comm. Internationale pour l'Exploration Scientifique de la Mer Méditerranée (CIESM)*, **38**, pp.79.

Colomina,I., Molina,P. (2014). Unmanned aerial systems for photogrammetry and remote sensing: A review. *ISPRS Journal of Photogrammetry and Remote Sensing*, **92**, pp. 79–97.

Connor, D.T., Martin, P.G., Smith, N.T., Payne, L., Hutson, C., Payton, O.D., Yamashiki, Y., Scott, T.B.(2017). Application of airborne photogrammetry for the visualisation and assessment of contamination migration arising from a Fukushima waste storage facility. *Journal of Environmental Pollution.* (Unpublished, Under Peer review).

Cronan, D.S., Varnavas, S.P. (1999). Metalliferous sediments off Milos, Hellenic volcanic arc. *Exploration and Mining Geology*, **8(3-4)**, pp.289-297.

Dando, P.R., Hughes, J.A., Leahy, Y., Taylor, L.J., Zivanovic, S. (1995a). Earthquakes increase hydrothermal venting and nutrient inputs into the Aegean. *Continental Shelf Res*earch, **15**, pp.655–662.

Dando, P.R., Hughes, J.A., Leahy, Y., Niven, S.J., Taylor, L.J., Smith, C. (1995b). Gas venting rates from submarine hydrothermal areas around the island of Milos, *Hellenic Volcanic Arc. Continental Shelf Research,* **15**, pp.913–929.

Dando PR, Hughes JA, Thiermann F. (1995c). Preliminary observations on biological communities at shallow hydrothermal vents in the Aegean Sea. Hydrothermal Vents and Processes, *Geological Society Special Publication,* **87**, pp.303-317.

Dando, P.R., Hughes, J.A., Leahy, Y., Niven, S.J., Taylor, L.J. and Smith, C. (1995d). Gas venting rates from submarine hydrothermal areas around the island of Milos, Hellenic Volcanic Arc. *Continental Shelf Research*, **15(8)**, pp.913-929.

Dando, P., Linke, P., Karnassopoulou, A. (1999) Echosounder Surveys in: Meteor - Berichte 99-2 Mittelmeer 1997/98 Cruise No. 40, pp. 45-46.

Dando, P. R., Aliani, S., Arab, H., Bianchi, C. N., Brehmer, M., Cocito, S., Fowler, S. W., Gundersen, J., Hooper, L. E., Kölbl, R., Kuever, J., Linke, P., Makropoulos, K. C., Meloni, R., Miquel, J.-C., Morri, C., Müller, S., Robinson, C., Schlesner, H., Sievert, S., Stöhr, R., Stüben, D., Thomm, M., Varnavas, S. P., Ziebis, W. (2000). Hydrothermal studies in the Aegean Sea. *Physics and Chemistry of the Earth* (B), **25**, pp.1-8.

Dando, P. R. (2010) Biological communities at marine shallow-water vent and seep sites, in: Kiel, S. (Ed.) The vent and seep biota – from microbes to ecosystems. *Topics in Geobiology,* **33**, pp.333-378, 477-478.

Drap, P. (2012). Underwater photogrammetry for archaeology. In *Special Applications of Photogrammetry*. InTech.

Fitzsimons, M.F., Dando, P.R., Hughes, J.A., Thiermann, F., Akoumianaki, I., Pratt, S.M. (1997). Submarine hydrothermal brine seeps off Milos, Greece. Observations and geochemistry. *Marine Chemistry*, **57(3-4),** pp.325-340.

Fytikas, M., Markopoulos, T. (2000). Fieldtrip to Milos guidebook. Institute of geology and mineral exploration. Silver & Barite ores mining Co.S.A and IGME, for the mineral policy sector group (MPS) of the Eurogeosurveys and the society for geology applied to mineral deposits (SGA).

Fytikas, M., Marinelli, G.(1976). Geology and geothermics of the island of Milos (Greece). International Congress on Thermal Waters, Geothermal Energy and Volcanism of the Mediterranean Area, Institute of Geology and Mineral Exploration. pp.58.

Fytikas M. (1977). 1:25 000 Geological Map of Milos. Institute of Geology and Mineral Exploration, Greece.

Fytikas, M., Innocenti, F., Kolios, N., Manetti, P., Mazzuoli, R., Poli, G., Rita, F., Villari, L.(1986). Volcanology and petrology of volcanic products from the island of Milos and neighbouring islets. *Journal of Volcanology and Geothermal Research*, **28(3-4),** pp.297-317.

Fytikas, M., Innocenti, F., Manetti, P., Peccerillo, A., Mazzuoli, R., Villari, L. (1984). Tertiary to Quaternary evolution of volcanism in the Aegean region. *Geological Society*, London, Special Publications, **17(1),** pp.687-699.

Gilhooly, W.P., Fike, D.A., Druschel, G.K., Kafantaris, F.C.A., Price, R.E., Amend, J.P. (2014). Sulfur and oxygen isotope insights into sulfur cycling in shallow-sea hydrothermal vents, Milos, Greece. *Geochemical transactions*, ***15*(1),** pp.12.

Gonçalves, J.A., Henriques, R. (2015). UAV photogrammetry for topographic monitoring of coastal areas. *ISPRS J. Photogramm. Remote Sens.* **104**, pp.101–111.

Innocenti F, Manetti P, Peccerilo A, Poli,G. (1979). Inner arc volcanism in NW Aegean arc: geochemical and geochronological data. Bulletin of Volcanology, **44,** pp.145–158.

Jackson, J.A. (1994). *Active tectonics of the Aegean region.* Annual Review of Earth and Planetary Sciences. **22**, pp.239–271.

Liakopoulos, A., Glasby, G.P., Papavassiliou, C.T., Boulegue, J.(2001). Nature and origin of the Vani manganese deposit, Milos, Greece: an overview. *Ore Geology Reviews*, **18(3)**, pp.181-209.

Mendrinos, D., Ioannis, C., Polyzou, O., Karytsas, C. (2010). Exploring for geothermal resources in Greece. *Geothermics*, **39**, pp.124-137.

Naden J., Kilias S.P., Darbyshire D.P.F. (2005). Active geothermal systems with entrained seawater as modern analogs for transitional volcanic-hosted massive sulfide and continental magmato-hydrothermal mineralization: The example of Milos Island, Greece. *Geology*. **33**, pp.541-544.

Nomikou, P., Papanikolaou, D., Alexandri, M., Sakellariou, D., Rousakis, G. (2013). Submarine volcanoes along the Aegean volcanic arc. *Tectonophysics*, **597-598**, pp. 123-146.

Nomikou, P., Carey, S., Papanikolaou, D., Croff, Bell K., Sakellariou, D., Alexandri, M., Bejelou, K.(2012). Submarine volcanoes of the Kolumbo volcanic zone NE of Santorini Caldera, Greece. *Global and Planetary Change,* **90–91**, pp.135–151.

Nomikou, P., Papanikolaou, D., Alexandri, M., Sakellariou, D., Rousakis, G.(2013). Submarine volcanoes along the Aegean volcanic arc. *Tectonophysics*, **597**, pp.123-146.

Papanikolaou, D., Lekkas, E., Syskakis, D. (1990). Tectonic analysis of the Milos geothermal field. Bulletin of the Geological Society of Greece XXIV, pp.27–46.

Papanikolaou, D., Lekkas, E., Syskakis, D., Adamopolou, E.(1993). Correlation on neotectonic structures with the geodynamic activity in Milos during the earthquakes of March 1992.Geol. Soc. Greece, **28,** pp.413–428.

Robinson C, Ziebis W, Müller S, Eichstadt K, Dando P, Linke P, Varnavas S, Megalovasilis P, Panagiotaras D.(1997). In situ investigations of shallow water hydrothermal vent systems, Palaeochori Bay, Milos, Aegean Sea. *Proceedings of the 4th Underwater Science Symposium. Society for Underwater Technology*, Newcastle upon Tyne, pp.85-100.

Sievert, S.M., Brinkhoff, T., Muyzer, G., Ziebis, W. and Kuever, J.(1999). Spatial heterogeneity of bacterial populations along an environmental gradient at a shallow submarine hydrothermal vent near Milos Island (Greece). *Applied and environmental microbiology*, **65(9),** pp.3834-3842.

Sigurdsson, H., Carey, S., Alexandri, M., Vougioukalakis, G., Croff, K.L., Roman, C., Sakellariou, D., Anagnostou, C., Rousakis, G., Ioakim, C., Gogou, A., Ballas, D., Misaridis, T., Nomikou, P., (2006). Marine investigations of Greece's Santorini volcanic field. *Eos,* **87 (34),** pp.337–339.

Snavely, N., Seitz, S.N., Szeliski, R.(2008).Modeling the world from internet photo collections. *International Journal of Computer Vision,* **80**, pp.189–210.

Stewart, A.L., McPhie, J.(2006). Facies architecture and Late Pliocene–Pleistocene evolution of a felsic volcanic island, Milos, Greece. *Bulletin of Volcanology*, ***68*(7-8)**, pp.703-726.

Teague, J., Scott, T., Allen, M.J. (2017). The use of Low-Cost ROV for Deep-Sea Mineral and Ore Prospecting. *Journal of Ocean Engineering*. (Unpublished, Under Peer review)

Teague, J., Scott, T. (2017). Underwater Photogrammetry and 3D reconstruction of submerged objects in shallow environments by ROV as an alternative method to Lidar and Sonar. *Journal of Marine Science Research and Technology*. (Unpublished, Under Peer review)

Triggs, B., McLauchlan, P.F., Hartley, R.I., Fitzgibbon, A.W. (2000). Bundle Adjustment — A Modern Synthesis. *Vis. Algorithms Theory Pract. 1883*, pp.153–177.

Valsami-Jones, E., Baltatzis, E., Bailey, E.H., Boyce, A.J., Alexander, J.L., Magganas, A., Anderson, L., Waldron, S., Ragnarsdottir, K.V. (2005). The geochemistry of fluids from an active shallow submarine hydrothermal system: Milos island, Hellenic Volcanic Arc. *Journal of Volcanology and Geothermal Research*, **148(1)**, pp.130-151.

 doi:10.20944/preprints201710.0014.v2

WaterLinked.(2017). *APS100 + GPS = UNDERWATER GPS.*[Online] Available at: https://waterlinked.com.(Accessed 9 October 2017).

Westoby, M.J., Brasington, J., Glasser, N.F., Hambrey, M.J., Reynolds, J.M. (2012). 'Structure-from-Motion' photogrammetry: a low-cost, effective tool for geoscience applications. *Geomorphology*, **179**, pp.300–314.

Yücel, M., Sievert, S.M., Vetriani, C., Foustoukos, D.I., Giovannelli, D., Le Bris, N. (2013). Eco-geochemical dynamics of a shallow-water hydrothermal vent system at Milos Island, Aegean Sea (Eastern Mediterranean). *Chemical Geology*, **356**, pp.11-20.